SIAM J. NUMER. ANAL.
Vol. 57, No. 2, pp. 681–701

NUMERICAL APPROXIMATION OF THE BEST DECAY RATE FOR SOME DISSIPATIVE SYSTEMS*

KAÏS AMMARI† AND CARLOS CASTRO‡

Abstract. We propose a projection method to approximate the spectrum of a dissipative system which is a bounded perturbation of a skew-adjoint operator. We show that the associated discrete spectra approximate the frequencies of the continuous problem uniformly with respect to the discretization parameter, up to a fixed number that can be estimated a priori. Based on this result we introduce an algorithm to approximate the spectral abscissa and, therefore, the decay rate, for a large class of dissipative systems. As an application we analyze its dependence on the damping location in several hyperbolic damped systems.

Key words. eigenvalue approximation, projection method, rate of decay, spectral abscissa, dissipative system

AMS subject classifications. 74K10, 35Q72, 35B40

DOI. 10.1137/17M1160057

1. Introduction.

Given an evolution dissipative system on a Hilbert space $\mathcal{H}$ with norm $\|\cdot\|$ we define the best decay rate as

$$\inf\{\omega : \exists C(\omega) > 0 \text{ s.t. } \|u(t)\| \leq C\|u(0)\|e^{\omega t} \text{ for every finite energy solution}\}. \tag{1.1}$$

The characterization of this best decay rate is a difficult problem and does not have a complete answer in the general case. In the particular case of a hyperbolic system perturbed with a damping term this question has been addressed by many authors with different techniques (see [3], [4], [6], [9], [10], [12], and the references therein). These references correspond to 1-dimensional (1-D) problems for which the best decay rate is usually associated with the spectral abscissa of the generator of the semigroup, i.e., the supremum of the real part of their corresponding eigenvalues. For higher dimensions the spectral abscissa also plays a role. In [18] Lebeau characterized the value of the best decay rate for the damped wave equation in terms of two quantities: the spectral abscissa and the mean value of the damping coefficient along the rays of geometrical optics.

In principle, the spectral abscissa should be easier to compute than the best decay rate, since the latter requires a characterization of the asymptotic behavior of all possible solutions. However, when considering distributed systems (as wave or beam models), the numerical approximation of the spectrum is not an easy task. For example, if we consider natural approaches based on computing the spectral abscissa of finite element or finite difference approximations the method fails. This is due to the numerical dispersion introduced by these methods at the high frequencies that, in particular, severely affect the approximation of large eigenvalues. This phenomenon has been largely studied in different contexts specially related with the numerical

*Received by the editors December 6, 2017; accepted for publication (in revised form) January 22, 2019; published electronically March 26, 2019.
http://www.siam.org/journals/sinum/57-2/M116005.html
Funding: The work of the second author was supported by grant MTM2017-85934-C3-3-P from the MICINN (Spain).
†Mathematics, University of Monastir, Monastir, 5019, Tunisia (kais.ammari@fsm.rnu.tn).
‡Matemática e Informática Aplicadas a la Ingeniería Civil, Universidad Politécnica de Madrid, Madrid, 28040, Spain (carlos.castro@upm.es).

approximation of control and stabilization problems for hyperbolic models (see, for example, [25], [13], [11], [14]). Most of the cures proposed so far are based on Tychonoff regularization (see [13], [21]), filtering techniques for the high frequencies (see [17]), multigrid techniques (see [19]), or mixed finite element methods (see [7] and [8]). But none of these techniques seems to provide a uniform approximation of the whole spectrum, required to obtain the spectral abscissa. It is important to highlight that here the problem is not that the large frequencies of these discrete approximations are difficult to compute numerically. Of course this could be also the case but this is not the difficulty that we address here. The challenge is that, even if we are able to compute them exactly, they are not close to those of the continuous model. In particular, linear algebra techniques do not seem useful in this context.

Note however that, even if the whole spectrum of the discrete approximation is not close to the continuous one, we can derive a strategy to obtain a partial approximation, by removing the high frequencies from the finite element model (or the finite differences one). This was the idea followed by Asch and Lebeau in [5] for the 2-dimensional (2-D) damped wave equation. But, how many frequencies do we have to remove in order to have a good approximation? This is completely unclear in general. To have an idea, we consider the simplest example of the 1-D undamped wave equation in the interval $x \in (0,1)$. The associated eigenvalues are $\lambda_k = ik\pi$, $k \in \mathbb{Z}^*$, while the finite element approximation with uniform mesh provides $\lambda_k^N = i2N \sin(\frac{k\pi}{2N})$, where N is the number of elements. Assume that we want an ε-approximation of the k frequency, i.e.,

$$\left| ik\pi - i2N \sin\left(\frac{k\pi}{2N}\right) \right| \leq \varepsilon.$$

Then, using a Taylor expansion of the $\sin(x)$ near $x = 0$, we easily obtain an estimate of N,

$$N \sim \frac{k^{3/2}\pi^{3/2}}{2\sqrt{6}\sqrt{\varepsilon}}.$$

In particular, N grows as $k^{3/2}$. For example, for the lower 20 frequencies, i.e., $|k| \leq 10$, with $\varepsilon = 0.1$ we have to compute the eigenvalues of a matrix with size around $(2N) \times (2N) \sim 440 \times 440$. Moreover, this estimate is only valid for this particular case where we know exactly the eigenvalues of the continuous problem. For more general non-self-adjoint operators we do not have such estimates. This illustrates the main two drawbacks of the finite element method: (a) in general, we cannot give an estimate of the size of the discretization parameter N to approximate the first k frequencies with a given error ε; and (b) it is not very efficient to approximate large eigenvalues since, in one of the simplest cases where we can compute this N, it requires $N \sim k^{3/2}\varepsilon^{-1/2}$.

Note that the main obstacle to obtaining better approximations with the finite element method is the dispersion of the higher frequencies produced by the numerical scheme. Similar dispersion formulas hold in other finite element and finite difference schemes (see for example [16, Chap. 9], for an analysis of the dispersion in finite element approximations and [22, Chap. 5], for the finite difference one), even higher order ones (see [23]). In these references, the dispersion is computed for the Laplace operator and it severely affects the high frequencies in all the cases. Moreover, it is unclear how to extend this dispersion analysis, based on the Fourier representation of discrete solutions, when considering perturbed operators as in this paper.

Here we propose a more efficient method to approximate the spectrum of dissipative systems which are a bounded perturbation of unbounded skew-adjoint operators. Roughly speaking, it consists of a projection method on finite dimensional subspaces

generated by the first eigenfunctions of the unperturbed operator. This can be interpreted as a Bubnov–Galerkin method. Convergence and error estimates for such methods are well known when the underlying operator is self-adjoint (see [24]), but the techniques cannot be extended to our case.

As far as we know, the convergence of such projection methods in this context was considered for the first time by Osborn to approximate a finite number of eigenvalues when the unperturbed operator is self-adjoint (see [20]). In the present situation, we deal with perturbations of skew-adjoint operators but the result is easily generalized. We show that, under certain hypotheses, this analysis can be adapted to give a uniform approximation of the spectrum, up to a finite number of frequencies and, therefore, it can be used to approximate the spectral abscissa of the continuous model from the discrete one. In particular, we give an algorithm to approximate this spectral abscissa. The main drawback of this projection method is that it requires the computation of the eigenfunctions of the unperturbed operator. However, this is well known for 1-D problems or higher dimensional ones in special domains (intervals or balls), where this method can be easily applied.

As an application of this method we give some numerical experiments where we show the behavior of the spectral abscissa for different operators under different damping locations.

The rest of the paper is divided as follows: In section 2 we describe an abstract setting for some dissipative systems where, under certain conditions, the decay rate can be described by the spectral abscissa. In section 3 we describe the numerical projection method and prove the main result stated in Theorem 3.1, i.e., the uniform convergence of the spectra up to a small number of frequencies. We also show how this result can be used to approximate the spectral abscissa. In section 4 we describe a matrix formulation for the numerical method. Finally, in section 5 we give several examples.

2. Abstract setting. Let A be an unbounded operator on a Hilbert space H with norm $\|\cdot\|_H$. We assume that A is self-adjoint, positive, and with compact inverse. We denote its domain by $\mathcal{D}(A) \subset H$. Associated with A we consider $H_{\frac{1}{2}} = \mathcal{D}(A^{\frac{1}{2}})$, the scaled Hilbert space with the norm $\|z\|_{\frac{1}{2}} = \|A^{\frac{1}{2}} z\|_H \ \forall z \in H_{\frac{1}{2}}$.

We set $\mathcal{H} := H_{\frac{1}{2}} \times H$, endowed with the inner product

$$\left\langle [f,g], [u,v] \right\rangle_{\mathcal{H}} := \langle A^{\frac{1}{2}} f, A^{\frac{1}{2}} u \rangle_H + \langle g, v \rangle_H \quad \text{for all } [f,g], [u,v] \text{ in } \mathcal{H},$$

and consider the first order differential equation

$$\begin{cases} \dot{Y}(t) = \mathcal{A}_{\mathcal{B}} Y(t), \\ Y(0) = Y_0 \in \mathcal{H}, \end{cases} \tag{2.1}$$

where $\mathcal{A}_{\mathcal{B}} := \mathcal{A}_0 - \mathcal{B} : \mathcal{D}(\mathcal{A}_{\mathcal{B}}) = \mathcal{D}(\mathcal{A}_0) \subset \mathcal{H} \to \mathcal{H}$ with

$$\mathcal{A}_0 = \begin{pmatrix} 0 & I \\ -A & 0 \end{pmatrix} : \mathcal{D}(\mathcal{A}_0) = \mathcal{D}(A) \times H_{\frac{1}{2}} \subset \mathcal{H} \to \mathcal{H},$$

and $\mathcal{B} \in \mathcal{L}(\mathcal{H})$ is a bounded operator satisfying

$$\left\langle \mathcal{B}Y, Y \right\rangle_{\mathcal{H}} \geq 0 \ \forall Y \in \mathcal{H}.$$

The operator $\mathcal{A}_0$ is skew-adjoint on $\mathcal{H}$ hence it generates a strongly continuous group of unitary operators on $\mathcal{H}$, denoted by $(\mathbf{S}_0(t))_{t\in\mathbb{R}}$. Since $\mathcal{A}_{\mathcal{B}}$ is dissipative and

onto, it generates a contraction semigroup on $\mathcal{H}$, denoted by $(\mathbf{S}_{\mathcal{B}}(t))_{t\in\mathbb{R}^+}$. Therefore system (2.1) is well-posed. Moreover, it is easy to prove that

$$\frac{1}{2}\|Y(0)\|^2_{\mathcal{H}} - \frac{1}{2}\|Y(t)\|^2_{\mathcal{H}} = \int_0^t \Big\langle \mathcal{B}Y(s), Y(s)\Big\rangle_{\mathcal{H}} ds \geq 0 \ \ \forall\, t \geq 0. \tag{2.2}$$

In particular, this means that the mapping $t \mapsto \|Y(t)\|^2_{\mathcal{H}}$ is not increasing. In many applications it is important to know if this mapping decays exponentially when $t \to +\infty$, i.e., if the system (2.1) is exponentially stable and, if so, what is the minimal rate. This motivates the definition of best decay rate given in (1.1),

A natural way to characterize this optimal decay rate is through the spectrum of $\mathcal{A}_{\mathcal{B}}$, denoted by $\sigma(\mathcal{A}_{\mathcal{B}})$, since particular solutions associated with a single eigenfunction of $\mathcal{A}_{\mathcal{B}}$ will decay as the real part of the associated eigenvalue. Thus, if we define the spectral abscissa of the generator $\mathcal{A}_{\mathcal{B}}$ by

$$\mu(\mathcal{A}_{\mathcal{B}}) = \sup\big\{\mathrm{Re}(\lambda);\ \lambda \in \sigma(\mathcal{A}_{\mathcal{B}})\big\}, \tag{2.3}$$

then clearly

$$\mu(\mathcal{A}_{\mathcal{B}}) \leq \omega(\mathcal{B}). \tag{2.4}$$

Whether this spectral abscissa characterizes the optimal decay rate or not is an interesting question that can be answered in some particular situations. For example, this is true when the eigenfunctions associated with the operator $\mathcal{A}_{\mathcal{B}}$ constitute a Riesz basis for $\mathcal{H}$, since in this case all solutions can be written as a series of eigenfunctions.

Let us mention a particular example where this can be proved under certain hypotheses. Consider the damped second order system,

$$\begin{cases} \ddot{x}(t) + Ax(t) + BB^*\dot{x}(t) = 0, \\ \big(x(0), \dot{x}(0)\big) = (x_0, x_1) \in \mathcal{H} \end{cases} \tag{2.5}$$

with B a bounded operator from U to H, where $(U, \|\cdot\|_U)$ is another Hilbert space which will be identified with its dual.

By considering $Y(t) = (x(t), \dot{x}(t))^T$ we can write system (2.5) in the form (2.1) with

$$\mathcal{B} = \begin{pmatrix} 0 & 0 \\ 0 & BB^* \end{pmatrix} \in \mathcal{L}(\mathcal{H}).$$

The above system was considered in [2], and a sufficient condition to ensure the existence of a Riesz basis constituted by generalized eigenvectors of $\mathcal{A}_{\mathcal{B}}$ was given. The condition concerns the high frequencies of A. Let us denote the spectrum of A, $\sigma(A)$, by $\{\mu_j\}_{j\geq 1}$ with

$$0 < \mu_1 \leq \mu_2 \leq \mu_3 \leq \cdots \leq \mu_n \leq \cdots \to +\infty.$$

For $k \in \mathbb{N}^*$, we define $\delta_{\pm k} := |\pm i(\sqrt{\mu_{k+1}} - \sqrt{\mu_k})| = \sqrt{\mu_{k+1}} - \sqrt{\mu_k}$. We introduce the following assumptions:

(A1) $\lim_{k\to+\infty} \delta_k = +\infty$;

(A2) $(\frac{\delta_{k+1}}{\delta_k^2})_{k\geq 1} \in l^2(\mathbb{N}^*)$, where $l^2(\mathbb{N}^*)$ is the space of square integrable sequences.

Remark 2.1. Observe the following:

(i) The assumption (A1) implies that the high frequencies of $\mathcal{A}_0$ are simple.

(ii) Assumption (A2) implies

$$\lim_{k\to+\infty} \left(\frac{\delta_{k+1}}{\delta_k^2}\right) = 0. \tag{2.6}$$

(iii) Note that, in general, assumption (A2) does not imply hypothesis (A1).

THEOREM 2.2 (see [2]). *Assume* (A1) *and* (A2) *hold. Then,*

(i) *the eigenvectors of the associated operator $\mathcal{A}_\mathcal{B}$ corresponding to system* (2.5) *form a Riesz basis in the energy space $\mathcal{H}$;*

(ii)

$$\omega(\mathcal{B}) = \mu(\mathcal{A}_\mathcal{B}). \tag{2.7}$$

For the abstract-Schrödinger equation,

$$\begin{cases} \dot{z}(t) + iAz(t) + BB^*z(t) = 0 \ \forall\, t > 0, \\ z(0) = z_0, \end{cases} \tag{2.8}$$

we have the same result as in Theorem 2.2 (see [2]).

COROLLARY 2.3. *Assume*

(A3) $\lim_{k\to+\infty} \delta'_k := \mu_{k+1} - \mu_k = +\infty$

and

(A4) $(\frac{\delta'_{k+1}}{(\delta'_k)^2})_{k\geq 1} \in l^2(\mathbb{N}^*)$.

Then,

(i) *the eigenvectors of the associated operator $A_B := -iA - BB^*$ corresponding to system* (2.8) *form a Riesz basis in the energy space H;*

(ii)

$$\omega(B) = \mu(A_B). \tag{2.9}$$

3. Numerical aproximation of the spectrum. In this section we consider a projection method to approximate numerically the spectral abscissa of $\mathcal{A}_\mathcal{B}$, i.e., $\mu(\mathcal{A}_\mathcal{B})$. This projection method has been used previously to approximate a single eigenvalue, or a fixed number of them, in [20], when $\mathcal{A}_\mathcal{B}$ is a bounded perturbation of a self-adjoint operator. In the present situation, $\mathcal{A}_\mathcal{B} = \mathcal{A}_0 - \mathcal{B}$ with $\mathcal{A}_0$ skew-adjoint and $\mathcal{B}$ bounded, but the result is easily adapted to this case. We claim that, under certain hypotheses, this analysis provides a uniform approximation of almost the whole spectra and therefore it can be used to approximate the spectral abscissa of the continuous model from the discrete one. In fact, we give below an algorithm to obtain this approximation.

Throughout this section we assume that all the eigenvalues of A, that we denote by $\{\mu_k\}_{k\geq 1}$, are simple and ordered increasingly. We also denote by $\{v_k\}_{k\geq 1}$ the associated eigenvectors, that we assume normalized in the norm of H. In this case, the eigenvalues of $\mathcal{A}_0$ and the corresponding eigenvectors are given by

$$\mathcal{A}_0 V_k = \lambda_k V_k, \ \textit{where } V_k = \frac{v_k}{\sqrt{2}}\left[\frac{1}{\lambda_k}, 1\right] \quad \text{for all} \quad k \in \mathbb{Z}^*, \tag{3.1}$$

and $v_{-n} = v_n$, $\lambda_{\pm n} = \pm i\sqrt{\mu_n}$ for $n \in \mathbb{N}^*$. Moreover, the family $(V_{\pm k})_{k\in\mathbb{N}^*}$ is an orthonormal basis of the energy space $\mathcal{H}$.

Let us consider the finite dimensional approximation of $\mathcal{H}$ spanned by the first eigenfunctions of $\mathcal{A}_0$, i.e.,

$$\mathcal{H}^N = span\{V_k\}_{k\in Z_N^*},$$

where $Z_N^* = \{k \in \mathbb{Z}^*,\ |k| \leq N\}$ and $P^N : \mathcal{H} \to \mathcal{H}^N$, the associated orthogonal projection.

We define the following Galerkin approximation of the eigenvalue problem (3.1): find $\lambda \in \mathbb{C}$ such that there exists a solution $W^N \in \mathcal{H}^N$, $W^N \neq 0$, of the system

$$P^N \mathcal{A}_{\mathcal{B}} W^N = \lambda W^N. \tag{3.2}$$

The spectrum of $P^N \mathcal{A}_{\mathcal{B}}$ is denoted by $\sigma(P^N \mathcal{A}_{\mathcal{B}})$ and contains $2N$ eigenvalues counting multiplicity. Associated with this finite dimensional spectral problem we define the spectral abscissa,

$$\mu(P^N \mathcal{A}_{\mathcal{B}}) = \max\big\{\mathrm{Re}(\lambda);\ \lambda \in \sigma(P^N \mathcal{A}_{\mathcal{B}})\big\}. \tag{3.3}$$

Our main objective is to relate $\mu(P^N \mathcal{A}_{\mathcal{B}})$ with $\mu(\mathcal{A}_{\mathcal{B}})$. Obviously the most we can expect is that $\mu(P^N \mathcal{A}_{\mathcal{B}})$ approximates the spectral abscissa of the lower N frequencies of $\mathcal{A}_{\mathcal{B}}$. This is basically the statement in Theorem 3.1 below. Note, however, that this is not enough to approximate the spectral abscissa of $\mathcal{A}_{\mathcal{B}}$, unless this is given by one of the first N frequencies.

In practice, there are a number of situations where the large frequencies of $\mathcal{A}_{\mathcal{B}}$ exhibit an asymptotic behavior, in such a way that their real part approaches a specific value as the frequencies grow. In this case, we only have to consider N sufficiently large to reach this asymptotic regime. Based on this idea we propose below an algorithm to approximate $\mu(\mathcal{A}_{\mathcal{B}})$.

Before stating the main result of this section we introduce some notation that is used in the rest of the paper.

We denote by $\{(\nu_k, U_k)\}_{k\in\mathbb{Z}^*}$ (respectively, $\{(\eta_k^N, W_k^N)\}_{k\in\mathbb{Z}^*}$) the eigenvalues and associated eigenvectors of $\mathcal{A}_{\mathcal{B}}$ (respectively, $P^N \mathcal{A}_{\mathcal{B}}$), that we assume ordered in such a way that $Im(\nu_k) \leq Im(\nu_{k+1})$ and, when equal, $|\nu_{k+1}| \leq |\nu_k|$ (respectively, $Im(\eta_k^N) \leq Im(\eta_{k+1}^N)$). Note that this is the same ordering chosen for the eigenvalues $\{\lambda_k\}_{k\in\mathbb{Z}^*}$ of $\mathcal{A}_0$. We also assume that the above eigenvectors are normalized.

Finally, to simplify the notation, in this section we omit the space in the norms when there is no confusion, i.e., we consider $\|\cdot\| = \|\cdot\|_{\mathcal{H}}$ and $\|\cdot\| = \|\cdot\|_{\mathcal{L}(\mathcal{H})}$.

THEOREM 3.1. *Assume that the following hypotheses are satisfied:*

(H1) $\mathcal{A}_0 : D(\mathcal{A}_0) \subset \mathcal{H} \to \mathcal{H}$ *is skew-adjoint with simple eigenvalues* $\{\lambda_n\}_{n\in\mathbb{Z}^*}$.

(H2) *The eigenvalues of* $\mathcal{A}_0$ *satisfy the following:*

$$|\lambda_{j+1} - \lambda_j| > 2\|\mathcal{B}\| \text{ for all } j \in \mathbb{Z}^*.$$

(H3) $\|\mathcal{B}\| \leq |\lambda_1|$.

(H4) *The eigenvectors of* $\mathcal{A}_{\mathcal{B}} = \mathcal{A}_0 + \mathcal{B}$ *constitute a Riesz basis of* $\mathcal{H}$, *i.e., there exist constants* $m, M > 0$ *such that*

$$m \sum_{j\in\mathbb{Z}^*} |c_j|^2 \leq \left\| \sum_{j\in\mathbb{Z}^*} c_j U_j \right\|_{\mathcal{H}}^2 \leq M \sum_{j\in\mathbb{Z}^*} |c_j|^2 \quad \text{for all } \{c_j\} \in l^2. \tag{3.4}$$

(H5) *For each* $\varepsilon > 0$ *there exists* $r_1 > 0$ *such that*

$$\max_{|i|\leq p} \sum_{|j|\geq p+r_1} |<\mathcal{B}V_i, V_j>|^2 < \varepsilon \text{ for all } p > 0. \tag{3.5}$$

Then, given $\varepsilon > 0$ *there exists* $r > 0$ *independent of* N, *such that, for all* $N > r$,

$$\min_j |\eta_p^N - \nu_j| \leq 2\varepsilon \quad \text{for all } |p| \leq N - r, \tag{3.6}$$

$$\min_j |\eta_j^N - \nu_p| \leq 2\varepsilon \quad \text{for all } |p| \leq N - r. \tag{3.7}$$

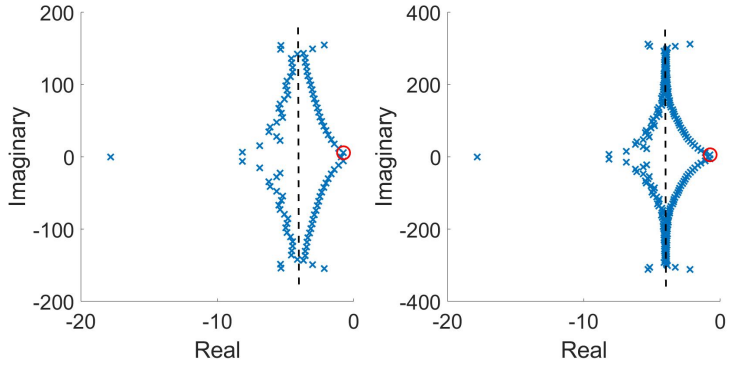

FIG. 1. *Numerical approximation of the spectrum of the 1-D damped wave equation in the interval $x \in (0,1)$ with a constant damping term $a(x) = 10\chi_{(0.1,0.5)}(x)$, the characteristic function of the interval $(0.1, 0.5)$, when considering $N = 50$ (left) and $N = 100$ (right). The eigenvalue that provides the spectral abscissa is circled. There are no explicit formulas for the continuous eigenvalues but it is known that the asymptotic spectral abcissa is given by $\alpha = -4$, in the dashed line. We observe that the highest frequencies exhibit a clear deviation from the asymptotic behavior of the continuous spectrum. However this only happens for a fixed number of frequencies that does not depend on N.*

Remark 3.2. Theorem 3.1 establishes the uniform convergence of the discrete spectrum, as $N \to \infty$, up to the highest $2r$ ones. As we show in the proof below, the value of r in the statement of Theorem 3.1 depends on the value r_1 in hypotheses (H5) and the asymptotic gap of the eigenvalues of the unperturbed operator, i.e., $|\lambda_{j+1} - \lambda_j|$ for large $|j|$. Therefore, it can be computed without knowing the eigenvectors of $\mathcal{A}_\mathcal{B}$. It can be also estimated numerically for each specific example. In practice (at least in the experiments considered below) this value is small and only a few frequencies must be removed to have uniform convergence. In Figure 1 we show an example for the damped wave equation. In this example r is around 4 and we observe that this value does not increase for larger values of N.

Remark 3.3. Hypotheses (H2) and (H3) in Theorem 3.1 concern the unperturbed operator so that we can check them without knowing the spectrum of $\mathcal{A}_\mathcal{B}$. On the other hand, they are used in a technical part of the proof and can be probably relaxed, as checked in the numerical experiments below. The hypothesis (H4) is more involved since it usually requires some information of the spectrum of $\mathcal{A}_\mathcal{B}$. However, the standard technique to prove such a property for 1-D problems requires basically the asymptotics of the spectrum (see, for instance, [9]), that is usually known in a number of cases. Finally, hypotheses (H5) is a measure of the nondiagonality of the operator $\mathcal{B}$ with respect to the basis of eigenvectors for $\mathcal{A}_0$, and can be computed easily.

Before giving the proof of Theorem 3.1 we show how this result can be used to approximate $\mu(\mathcal{A}_\mathcal{B})$ from $\mu(P^N \mathcal{A}_\mathcal{B})$.

COROLLARY 3.4. *Assume that the hypotheses* (H1)–(H5) *in Theorem* 3.1 *are satisfied, together with the following one:*

(H6) *Given $\varepsilon > 0$, there exists N_1 and $\alpha \in \mathbb{R}$ such that*

$$| \, Re \, (\nu_k) - \alpha| \leq \varepsilon \quad \text{for all } |k| > N_1. \tag{3.8}$$

Let us define the following modified spectral abscissa, where we remove the highest

frequencies,

$$\mu_r(P^N\mathcal{A}_\mathcal{B}) = \max_{|j|\leq N-r} \mathrm{Re}(\eta_j^N). \tag{3.9}$$

Then, for each $\varepsilon > 0$ there exists N_1 and r, independent of N, such that

$$|\mu(\mathcal{A}_\mathcal{B}) - \mu_r(P^N\mathcal{A}_\mathcal{B})| \leq \varepsilon \quad \text{for all } N > N_1. \tag{3.10}$$

Remark 3.5. The hypothesis (H6) above is satisfied in many interesting problems. What is more difficult is to find an estimate of N_1, since this value may change for each specific example. For example, it is well known that the damped wave equation, that we describe below in the applications (see section 5.1), satisfies (H6) as soon as the damping distribution $a(x)$ is a bounded variation function. However, the value N_1 depends on $a(x)$ and, as far as we know, there are no estimates on this dependence that provide a criteria to choose N_1 a priori.

From this result we can easily implement an algorithm to obtain an approximation of the spectral abscissa:

Step 1. Choose $\varepsilon > 0$ and take N_1 from hypotheses (H6) above. This value N_1 may change from one case to other and, as commented on in Remark 3.5 above, it is difficult to give a priori criteria to compute it. In practice we can give a numerical estimate by chosing N sufficiently large in order to have that the real part of the last frequencies are sufficiently close.

Step 2. Compute the value r given by Theorem 3.1. As we have said, this can be computed without knowing the spectrum of $\mathcal{A}_\mathcal{B}$. Alternatively, it can also be estimated numerically for each specific example. For example, we choose N_0, not too large, and compare the spectra $\sigma(P^{N_0}\mathcal{A}_\mathcal{B})$ with $\sigma(P^{2N_0}\mathcal{A}_\mathcal{B})$. Then we can estimate r by the smallest value for which

$$|\eta_i^{N_0} - \eta_i^{2N_0}| \leq \varepsilon \quad \text{for all } |i| \leq N - r.$$

Step 3. Take $N > N_1 + r$ and compute $\mu_r(P^N\mathcal{A}_\mathcal{B})$ by removing the highest frequencies in $\mu(P^N\mathcal{A}_\mathcal{B})$. According to Corollary 3.4, this satifies (3.10).

In the rest of this section we prove Theorem 3.1.

Proof of Theorem 3.1. We divide the proof into several steps.

Step 1. Basic estimates. Here we prove a rough estimate of the eigenvalues. Let

$$C_m = \{\lambda \in \mathbb{C} \text{ such that } |\lambda - \lambda_m| < \|\mathcal{B}\|\}. \tag{3.11}$$

By hypothesis (H2), C_m are disjoint. On the other hand, following the perturbation argument in [20], one can prove that the number of eigenvalues, counting with algebraic multiplicity, of $\mathcal{A}_0, \mathcal{A}_\mathcal{B}$, and $P^N\mathcal{A}_\mathcal{B}$ in C_m coincide. In particular, C_m contains only one eigenvalue of $\mathcal{A}_0, \mathcal{A}_\mathcal{B}$, and $P^N\mathcal{A}_\mathcal{B}$, i.e.,

$$|\lambda_k - \nu_k|,\ |\lambda_k - \eta_k^N| < \|\mathcal{B}\| \quad \text{for all } k. \tag{3.12}$$

As a consequence, estimates (3.6) and (3.7) can be deduced one from the other. We focus on the proof of (3.6).

Step 2. We prove the following estimate,

$$\min_{j\in\mathbb{Z}^*} |\nu_j - \eta_p^N| \leq \sqrt{\frac{M}{m}} \|(I - P^N)\mathcal{B}W_p^N\| \quad \text{for all } |p| \leq N, \tag{3.13}$$

where the constants M and m are those given in (3.4).

As $\{U_j\}_{j\in\mathbb{Z}^*}$ constitutes a Riesz Basis for $\mathcal{H}$ we can write

$$W_p^N = \sum_{j\in\mathbb{Z}^*} \alpha_{p,j} U_j, \quad \alpha_{p,j} \in \mathbb{C}.$$

We have,

$$\sum_{j\in\mathbb{Z}^*} \alpha_{p,j} U_j(\eta_p^N - \nu_j) = P^N \mathcal{A}_\mathcal{B} W_p^N - \mathcal{A}_\mathcal{B} W_p^N = P^N(\mathcal{A}_0 - \mathcal{B})W_p^N - (\mathcal{A}_0 - \mathcal{B})W_p^N$$
$$= (I - P^N)\mathcal{B}W_p^N.$$

From this identity we have, on one hand,

$$\left\| \sum_{j\in\mathbb{Z}^*} \alpha_{p,j} U_j^N(\eta_p^N - \nu_j) \right\| \le \left\|(P^N - I)\mathcal{B}W_p^N\right\| \tag{3.14}$$

and, on the other hand,

$$\left\| \sum_{j\in\mathbb{Z}^*} \alpha_{p,j} U_j^N(\eta_p^N - \nu_j) \right\|^2 \ge m \sum_{j\in\mathbb{Z}^*} |\alpha_{p,j}|^2 |\eta_p^N - \nu_j|^2 \ge m \min_{j\in\mathbb{Z}^*} |\eta_p^N - \nu_j|^2 \sum_{j\in\mathbb{Z}^*} |\alpha_{p,j}|^2$$
$$= \frac{m}{M} \min_{j\in\mathbb{Z}^*} |\eta_p^N - \nu_j|^2,$$

where we have taken into account the normalization of W_p^N. Combining this inequality with (3.14) we easily obtain (3.13).

Step 3. To estimate the right-hand side of (3.13) we look at the contribution of the large Fourier coefficients of W_p^N in the basis $\{V_j\}_{j\in Z^*}$. In particular we prove that given $r, p_0 > 0$ such that $N - r < p_0 < N$, the following holds:

$$\|(I - P^{p_0})W_p^N\| \le \frac{\|\mathcal{B}\|}{|\lambda_{p_0+1} - \lambda_{N-r}| - \|\mathcal{B}\|} \text{ for all } |p| \le N - r. \tag{3.15}$$

In fact, we have

$$\|(I - P^{p_0})W_p^N\|^2 = \sum_{|j|\ge p_0+1} |\langle W_p^N, V_j\rangle|^2. \tag{3.16}$$

Now observe that

$$(\eta_p^N - \lambda_j)\left\langle W_p^N, V_j\right\rangle = \left\langle P^N \mathcal{A}_\mathcal{B} W_p^N, V_j\right\rangle - \left\langle W_p^N, (\mathcal{A}_0)^T V_j\right\rangle$$
$$= \left\langle (P^N \mathcal{A}_\mathcal{B} - \mathcal{A}_0)W_p^N, V_j\right\rangle = \left\langle (P^N(\mathcal{A}_0 - \mathcal{B}) - \mathcal{A}_0)W_p^N, V_j\right\rangle$$
$$= -\left\langle P^N \mathcal{B} W_p^N, V_j\right\rangle$$

and, taking the modulus in this inequality,

$$\left|\left\langle W_p^N, V_j\right\rangle\right|^2 \le \frac{\left|\left\langle P^N \mathcal{B} W_p^N, V_j\right\rangle\right|^2}{|\eta_p^N - \lambda_j|^2} \le \frac{\left|\left\langle P^N \mathcal{B} W_p^N, V_j\right\rangle\right|^2}{|\eta_{p_0+1}^N - \lambda_{N-r}|^2}$$
$$\le \frac{\left|\left\langle P^N \mathcal{B} W_p^N, V_j\right\rangle\right|^2}{(|\lambda_{p_0+1} - \lambda_{N-r}| - \|\mathcal{B}\|)^2}, \tag{3.17}$$

where we have used that $|p| \leq N - r < p_0$, and estimate (3.12) for $\eta_{p_0}^N$, since $N - r \geq m_0$. Therefore, substituting (3.17) into (3.16),

$$\sum_{|j|\geq p_0+1} |< W_p^N, V_j >|^2 \leq \sum_{|j|\geq p_0+1} \frac{\left|\left\langle P^N \mathcal{B} W_p^N, V_j \right\rangle\right|^2}{(|\lambda_{p_0+1} - \lambda_{N-r}| - \|\mathcal{B}\|)^2}$$
$$\leq \frac{\|P^N \mathcal{B} W_p^N\|^2}{(|\lambda_{p_0+1} - \lambda_{N-r}| - \|\mathcal{B}\|)^2} \leq \frac{\|\mathcal{B}\|^2}{(|\lambda_{p_0+1} - \lambda_{N-r}| - \|\mathcal{B}\|)^2},$$

which combined with (3.16) gives the desired estimate (3.15).

Step 4. Here we obtain (3.6). First of all, note that for p_0 satisfying $N - r > p_0 \geq m_0$, we have

$$\|(I - P^N)\mathcal{B} W_p^N\| \leq \|(I - P^N)\mathcal{B} P^{p_0} W_p^N\| + \|(I - P^N)\mathcal{B}(I - P^{p_0}) W_p^N\|$$
$$\leq \max_{|i|\leq p_0} \|(I - P^N)\mathcal{B} V_i\| + \|\mathcal{B}\| \, \|(I - P^{p_0}) W_p^N\|. \tag{3.18}$$

Given $\varepsilon > 0$, we choose p_0 such that the first term in the right-hand side of (3.18) is lower than $\varepsilon/2$. From hypothesis (H5) this can be done for p_0 satisfying

$$N - p_0 \geq r_1, \text{ for some } r_1 \text{ independent of } N. \tag{3.19}$$

Now we choose r such that the second term in the right-hand side of (3.18) is lower than $\varepsilon/2$ too. From (3.15) and hypothesis (H2) this can be done as long as

$$p_0 - (N - r) \geq r_2 \text{ for some } r_2 \text{ independent of } N. \tag{3.20}$$

Therefore, if we take $r \geq r_1 + r_2$, estimate (3.6) follows directly from (3.18). This concludes the proof of Theorem 3.1. ∎

Remark 3.6. As we show in the experiments below, hypotheses (H2) and (H3) in Theorem 3.1 are not optimal in the sense that the projection method provides good results for a large class of systems that do not satisfy them. Let us explain the difficulties in relaxing them in the above proof. They are used in Step 1 of the proof to obtain basic estimates between the eigenvalues of $\mathcal{A}_\mathcal{B}$ and those of $P^N \mathcal{A}_\mathcal{B}$. These estimates are derived by a perturbation argument with respect to the spectrum of the unperturbed operator $\mathcal{A}_0$, which is self-adjoint. Therefore, it is natural to have hypotheses on the size of the perturbation $\mathcal{A}_\mathcal{B} - \mathcal{A}_0 = \mathcal{B}$. In particular (H1)–(H2) allow us to assume that the sets C_m in (3.11) are disjoint and, in this sense, they are optimal. A direct perturbation argument between the eigenvalues of $\mathcal{A}_\mathcal{B}$ and those of $P^N \mathcal{A}_\mathcal{B}$, i.e., without using the spectrum of $\mathcal{A}_0$, would probably relax the hypotheses (H2)–(H3). However, spectral perturbation theory for non-self-adjoint operators, such as $\mathcal{A}_\mathcal{B}$, is a much more difficult issue. In particular, the perturbation argument used in Step 1 of the proof does not apply.

4. Matrix formulation of the numerical method. In this section we reduce the finite dimensional approximation of the eigenvalue problem (3.2) to a matrix eigenvalue problem, that we use later to implement the algorithm described in the previous section to approximate the spectral abscissa.

In order to write the finite dimensional eigenvalue problem (3.2) in matrix form we write

$$W^N = \sum_{k \in Z_N^*} c_k V_k$$

for some Fourier coefficients c_k. A straightforward computation shows that if we define

$$a_n = \frac{c_n}{\lambda_n} + \frac{c_{-n}}{\lambda_{-n}}, \qquad a_{N+n} = c_n + c_{-n}, \quad n = 1, 2, \dots, N,$$

then the eigenvalue problem (3.2) can be reduced to the equivalent matrix eigenvalue problem

$$M_N U^N = \lambda^N U^N, \quad U^N = (a_1, a_2, \dots, a_{2N})^T, \tag{4.1}$$

where I_N is the N-dimensional identity matrix,

$$M_N = \begin{pmatrix} 0 & I_N \\ -\Lambda_N & \Omega_N \end{pmatrix}, \quad \Lambda_N = \begin{pmatrix} \mu_1 & 0 & 0 & 0 \\ 0 & \mu_2 & 0 & 0 \\ \dots & \dots & \dots & \dots \\ 0 & 0 & 0 & \mu_N \end{pmatrix}, \quad \Omega_N = (\omega_{ij}),$$

and

$$\omega_{ij} = -\langle BB^* v_i, v_j \rangle_H.$$

The discrete spectral abscissa is defined as

$$\mu(P^N \mathcal{A}_{\mathcal{B}}) = \sup\{\mathrm{Re}\lambda^N;\ \lambda_N \in \sigma(M_N)\}. \tag{4.2}$$

5. Some applications. We give here some examples of dissipative systems which satisfy assumptions (A1) and (A2) or do not (see section 2 above) but for which we can deduce that the best decay rate can be identified as a spectral abscissa. Also, not all the examples satisfy the hypotheses of Theorem 3.1 but the numerical algorithm presented before provides a good result in all of them.

5.1. Damped wave equation. We consider the following system:

$$\partial_t^2 u(x,t) - \partial_x^2 u(x,t) + 2a(x)\partial_t u(x,t) = 0, \quad 0 < x < 1,\ t > 0, \tag{5.1}$$

$$u(0,t) = u(1,t) = 0, \quad t > 0, \tag{5.2}$$

$$u(x,0) = u^0(x), \quad \partial_t u(x,0) = u^1(x), \quad 0 < x < 1, \tag{5.3}$$

where $a \in BV(0,1)$ is nonnegative satisfying the following condition:

$$\exists\, c > 0 \text{ s.t. } a(x) \geq c \text{ a.e. in a nonempty open subset } I \text{ of } (0,1). \tag{5.4}$$

We define the energy of the solution u of (5.1)–(5.3), at time t, as

$$E\big(u(t)\big) = \frac{1}{2}\int_0^1 \left(\big|\partial_t u(x,t)\big|^2 + \big|\partial_x u(x,t)\big|^2\right) dx, \tag{5.5}$$

$$U = L^2(0,1),\ H = L^2(0,1),\ H_{\frac{1}{2}} = H_0^1(0,1),$$

$$\mathcal{D}(A) = H^2(0,1) \cap H_0^1(0,1),$$

$$\mathcal{H} = H_0^1(0,1) \times L^2(0,1),$$

$$A = -\frac{d^2}{dx^2}, \quad B\phi = B^*\phi = \sqrt{2a(x)}\phi \quad \forall \phi \in L^2(0,1).$$

So,

$$\mathcal{A}_0 = \begin{pmatrix} 0 & I \\ \frac{d^2}{dx^2} & 0 \end{pmatrix},\ \mathcal{A}_{\mathcal{B}} = \begin{pmatrix} 0 & I \\ \frac{d^2}{dx^2} & -2a(x) \end{pmatrix}.$$

The operator $\mathcal{A}_0$ is skew-adjoint, with compact inverse and the spectrum is given by $\sigma(\mathcal{A}_0) = \{\pm ik\pi, k \in \mathbb{N}^*\}$. Therefore, the hypotheses (A1) and (A2) are not fulfilled for this problem. However, according to [15], if a satisfies (5.4) then $\omega(\mathcal{B}) < 0$. Moreover, in this case it is well known that the spectral abscissa coincides with the decay rate (see [9]).

To approximate the spectral abscissa we follow the algorithm described above. This requires us to check the hypotheses (H1)–(H6). (H1) is clearly true, while (H2)–(H3) depend on the norm of $\mathcal{B}$. In this case,

$$\|\mathcal{B}\| \leq 2\|a\|_{L^\infty(0,1)},$$

and this is satisfied as soon as $\|a\|_{L^\infty(0,1)} < \pi/2$. Hypotheses (H4) and (H6) were proved for this damped wave equation in [9] under condition (5.4). In fact, the asymptotic spectral abcissa is given by $\alpha = -\int_0^1 a(x)dx$. Finally, hypotheses (H5) has to be checked for each specific example but, in general, it is easy to establish when $a(x)$ is a characteristic function of a subinterval $\omega \subset (0,1)$ or a finite linear combination of the eigenvectors of $\mathcal{A}_0$.

The eigenvalue problem is reduced to the matrix eigenvalue problem (4.1). In this case, $\mu_k = k^2\pi^2$ and

$$\omega_{jk} = -2\int_0^1 a(x)\sin(j\pi x)\sin(k\pi x)dx. \tag{5.6}$$

This matrix eigenvalue problem is solved with the MATLAB command *eig*. We recall that here we are not interested in the particular difficulties associated with this discrete eigenvalue problem. Our experiments below consider relatively small size problems to avoid possible numerical problems coming from the matrix structure.

In order to compare the method described in this paper with other possible approaches we first consider the particular case $a(x) = \chi_{(1/4,3/4)}(x)$, i.e., the characteristic function of the interval $(1/4, 3/4)$. In this case, all the hypotheses (H1)–(H6) are satisfied. Moreover, the asymptotic spectral abcissa in hypothesis (H6) is given by $\alpha = -\int_0^1 a(x)dx = -1/2$. We focus on the comparison with the finite element method. Other approaches based on finite differences or higher order methods provide similar results. In Figure 2 we show the spectra computed with the finite element method and the projection method described above. Some remarks are in order:

1. The real part of the high frequencies for the projection method are close to the expected asymptotic spectral abcissa $\alpha = -1/2$.
2. The highest frequencies of the finite element approximation exhibit a large deviation from the expected asymptotic spectral abcissa. Note that a finer mesh translates this deviation to the new highest frequencies, that obviously are far from those of the continuous model.
3. The spectral abcissa of the finite element approximation can be much larger than the one for the continuous model, due to the large deviation of the high frequencies. Moreover, the real part of the highest frequencies becomes close to zero and the number of such frequencies increases as the discretization is refined. The natural approach to overcome this difficulty consists of filtering the high frequencies, as implemented in [5]. However this is tricky since we do not know a priori where this deviation becomes relevant to remove these frequencies.
4. A well-known strategy to recover stability properties in discrete approximations of dissipative systems consists of adding some numerical viscosity,

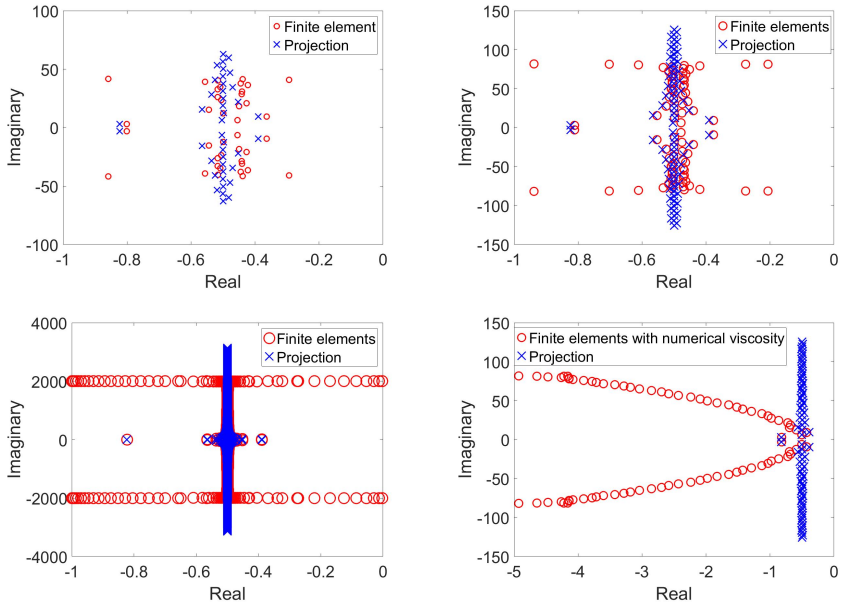

FIG. 2. *Numerical approximation of the spectra of the damped wave equation, when* $a(x) = \chi_{(1/4,3/4)}(x)$*, computed with the finite element method (circles) and the projection method introduced in this paper (crosses). The number of elements is* 20 *in the upper left figure,* 40 *in the upper right one, and* 1000 *in the lower left one. In the lower right graph the finite element method is modified by adding numerical viscosity.*

which corrects the loss of dissipation of the discrete large frequencies (see [21]). We followed this strategy to approximate the spectral abcissa. As showed in Figure 2 (lower right graph), the numerical viscosity pushes the high frequencies to the left part of the complex plane, leaving the spectral abcissa of the discrete system to the low frequencies. However, as we do not know what is the specific frequency that provides the spectral abcissa, it is difficult to quantify the effect of this dissipation on its numerical approximation. In other words, it is unclear how fine the discretization should be in order to guarantee that the frequency that provides the spectral abcissa is not overly dissipated, due to the numerical viscosity.

5. The main advantage of the projection algorithm described in section 3 is the uniform convergence of the spectra. For each $\varepsilon > 0$ there exists r such that we only have to remove the largest r frequencies to obtain an approximation of all the eigenvalues with error ε. Moreover, this value r is independent of N the number of frequencies considered in the projection method. In this particular experiment, for $\varepsilon = 10^{-2}$ the value is $r = 2$. This means that almost the whole spectra of the discrete model can be interpreted as a good perturbation of the continuous one. Note that the projection method requires filtering but, unlike the finite element method, we can estimate how many frequencies we have to filter and this number does not increase when considering a discrete model with more frequencies.

A practical property of the proposed method is that it allows one to obtain quickly the spectral abcissa for a large class of functions $a(x)$. Moreover, it is robust enough to give good results even when applied to systems that do not satisfy the hypotheses

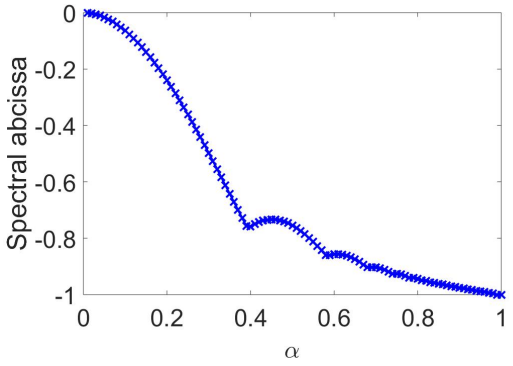

FIG. 3. *Spectral abscissa versus α for the damped wave equation when $a(x)$ is given by* (5.7) *and $x_0 = 0.5$.*

(H1)–(H6), and particularly hypotheses (H2)–(H3) that hold only when $\|a\|_{L^\infty(0,1)} < \pi/2$. This constitutes numerical evidence of the nonoptimality of hypotheses (H2)–(H3). The following experiments take advantage of this and analyze the behavior of the spectral abcissa in different situations.

In order to see how the distribution of the damping affects the spectral abscissa we consider several experiments. We take for $a(x)$ characteristic functions, so that (5.6) can be computed explicitly with $\int_0^1 a(s)ds = 1$ to maintain the same amount of damping. In this way we consider the following two-parametric family of dampings,

$$a(x) = \frac{1}{\alpha}\chi_{(x_0-\alpha/2,x_0+\alpha/2)}(x), \qquad x_0 \in (0,1/2),\ \alpha \in (0,2x_0]. \tag{5.7}$$

Here $x_0 \in (0,1/2]$ is the center of the support and $\alpha \in (0,2x_0]$ its length. For x_0 fixed and $\alpha \in (0,2x_0]$ we illustrate the effect of concentrating the damping around a single point. When α approaches zero we formally obtain a Dirac mass concentrated at x_0. In Figure 3 we show the dependence of the spectral abscissa on α when $x_0 = 1/2$. In particular this spectral abscissa becomes larger as $\alpha \to 0$ and smaller when $\alpha \to 1$ which corresponds to the constant case $a(x) = 1$. We also observe that the spectral abscissa is not monotone and that there are some values, around $\alpha = 0.4$ and $\alpha = 0.6$, for example, where it is not a differentiable function with respect to α. In the case $\alpha = 0.4$ this corresponds to the case where the spectral abscissa changes from the first to the second eigenvalue. We also observe the presence of several local minima.

Now, we fix the parameter $\alpha = 1/8$ and move the point $x_0 \in [1/4,1/2])$. Once again, the damping is a one-parametric family of characteristic functions with support in a segment of length $1/8$ that we move through the interval $(0,1)$. The idea is to understand how the location of the damping affects its efficiency. In Figure 4 we show the dependence of the decay on α. Note that lower spectral abscissa are obtained around the values $\alpha = 0.2,\ 0.4,\ 0.6$, and 0.8.

In Figure 5 we show the behavior of the spectral abscissa when we move both parameters. We see that the lower value corresponds to $(x_0,\alpha) = (1/2,1)$ which is when the damping is uniformly distributed in the interval $(0,1)$.

Another interesting example appears when the damping is a one-parametric family of a finite number of characteristic functions of the form

$$a(x) = \sum_{i=1}^{\beta} \frac{1}{2}\chi_{(\frac{2i-1}{2\beta}-\frac{1}{4i\beta},\frac{2i-1}{2\beta}-\frac{1}{4i\beta})}(x), \qquad \beta \in N. \tag{5.8}$$

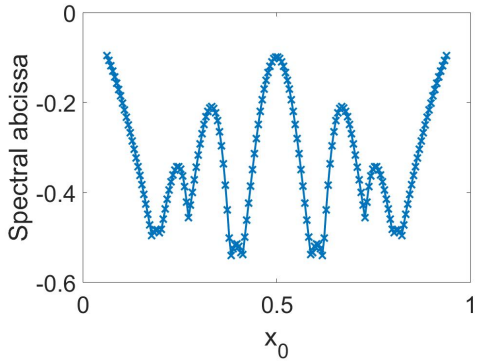

FIG. 4. *Spectral abscissa versus x_0 for the wave equation when $a(x)$ is given by* (5.7) *and* $\alpha = 1/8$.

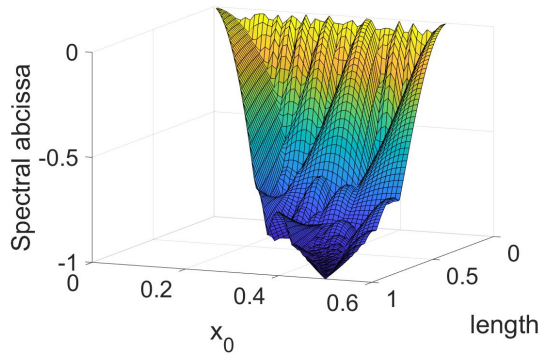

FIG. 5. *Spectral abscissa versus (x_0, α) for the wave equation when $a(x)$ is given by* (5.7).

Note that for larger β we consider a damping supported in an increasing number of intervals with lower length in such a way that the total amount of damping $\int_0^1 a(x)\,dx$ is conserved. In this way we try to understand the influence of an oscillating damping in the spectral abscissa. In Figure 6 we show the dependence of the spectral abscissa on β. We see that as we increase the number of intervals the spectral abscissa becomes larger.

A priori, this fragmentation of the support in the damping term could be interpreted as a good strategy to obtain better decay rates, since the damping support becomes dense in the domain. However, it is exactly the opposite since the spectral abcissa becomes larger.

5.2. Damped Euler–Bernoulli beam equation. We consider the following system:

$$\partial_t^2 u(x,t) + \partial_x^4 u(x,t) + 2a(x)\partial_t u(x,t) = 0, \quad 0 < x < 1,\ t > 0, \tag{5.9}$$

$$u(0,t) = u(1,t) = 0, \quad \partial_x^2 u(0,t) = \partial_x^2 u(1,t) = 0, \quad t > 0, \tag{5.10}$$

$$u(x,0) = u^0(x), \quad \partial_t u(x,0) = u^1(x), \quad 0 < x < 1, \tag{5.11}$$

where $a \in L^\infty(0,1)$ is nonnegative satisfying the following condition:

$$\exists\, c > 0 \text{ s.t. } a(x) \geq c \text{ a.e. in a nonempty open subset } I \text{ of } (0,1). \tag{5.12}$$

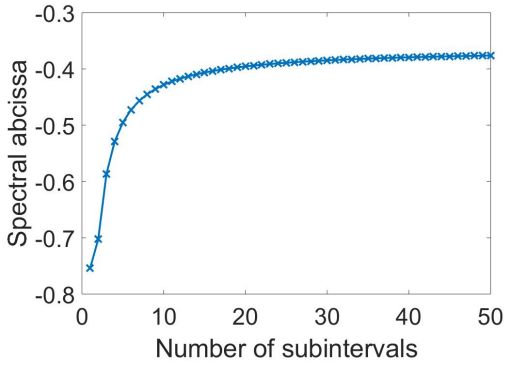

FIG. 6. *Spectral abscissa versus β (number of subintervals where the damping is supported) for the wave equation when $a(x)$ is given by* (5.8).

We define the energy of a solution u of (5.9)–(5.11), at time t, as

$$E\big(u(t)\big) = \frac{1}{2}\int_0^1 \Big(\big|\partial_t u(x,t)\big|^2 + \big|\partial_x^2 u(x,t)\big|^2\Big)\, dx, \tag{5.13}$$

$$U = L^2(0,1),\ H = L^2(0,1),\ H_{\frac{1}{2}} = H^2(0,1)\cap H_0^1(0,1),$$

$$\mathcal{D}(A) = \left\{u \in H^4(0,1)\cap H_0^1(0,1); \frac{d^2u}{dx^2}(0) = \frac{d^2u}{dx^2}(1) = 0\right\},$$

$$\mathcal{H} = [H^2(0,1)\cap H_0^1(0,1)]\times L^2(0,1),$$

$$A = \frac{d^4}{dx^4}, \quad B\phi = B^*\phi = \sqrt{2a(x)}\phi \quad \forall \phi \in L^2(0,1).$$

So,

$$\mathcal{A}_0 = \begin{pmatrix} 0 & I \\ -\frac{d^4}{dx^4} & 0 \end{pmatrix},\ \mathcal{A}_{\mathcal{B}} = \begin{pmatrix} 0 & I \\ -\frac{d^4}{dx^4} & -2a(x) \end{pmatrix}.$$

The operator $\mathcal{A}_0$ is skew-adjoint, with compact inverse and the spectrum given by $\sigma(\mathcal{A}_0) = \{\pm ik^2\pi^2, k \in \mathbb{N}^*\}$, then Assumptions (A1) and (A2) are satisfied. As a direct implication of Theorem 2.2, we have that the best decay rate is given by the spectral abscissa (this result was proved in [1]).

To approximate the spectral abscissa we introduce the numerical algorithm described above, where the eigenvalue problem is reduced to the matrix eigenvalue problem (4.1). In this case, $\mu_k = -k^4\pi^4$, $\lambda_k = \pm ik^2\pi^2$, and the hypotheses of Theorem 3.1 are satisfied for sufficiently small $a(x)$. More precisely, it is enough to consider $\|a\|_{L^\infty(0,1)} < \pi^2/2$.

Following the idea of the experiments for the wave equation we have considered the same damping functions $a(x)$. The results are completely analogous as can be seen in Figure 7.

5.3. Damped Schrödinger equation. We consider the following system:

$$\partial_t u(x,t) - i\,\partial_x^2 u(x,t) + a(x)u(x,t) = 0, \quad 0 < x < 1,\ t > 0, \tag{5.14}$$

$$u(0,t) = u(1,t) = 0, \quad t > 0, \tag{5.15}$$

$$u(x,0) = u^0(x), \quad 0 < x < 1, \tag{5.16}$$

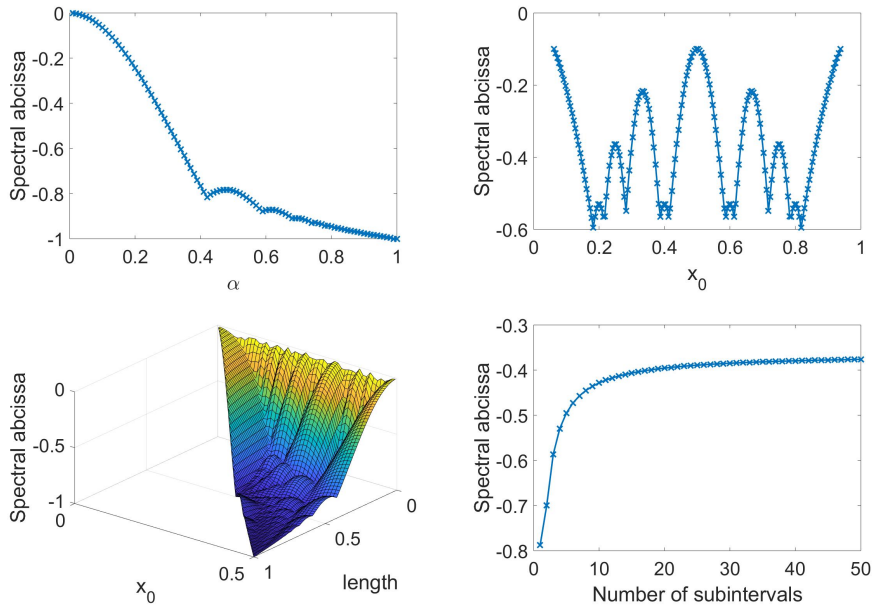

FIG. 7. *Spectral abscissa of the beam equation versus α for $x_0 = 1/2$ (upper left) versus x_0 for $\alpha = 1/8$ (upper right), versus (α, x_0) (lower left), when $a(x)$ is given by* (5.7)*, and versus the number of intervals β (lower right) when $a(x)$ is given by* (5.8).

where $a \in L^\infty(0,1)$ is nonnegative and satisfies the following condition: $\exists\, c > 0$ s.t. $a(x) \geq c$ a.e. in a nonempty open subset I of $(0,1)$.

We define the energy of a solution u of (5.14)–(5.16), at time t, as

$$E\big(u(t)\big) = \frac{1}{2}\int_0^1 \big|u(x,t)\big|^2\, dx\,. \tag{5.17}$$

In this case, we have

$$H = L^2(0,1), \qquad A = -\frac{d^2}{dx^2}, \qquad B = \sqrt{a(x)}\, I.$$

The operator iA is skew-adjoint and, with compact inverse and the spectrum given by $\sigma(iA) = \{\pm ik^2\pi^2, k \in \mathbb{N}^*\}$, then Assumptions (A1) and (A2) are satisfied. As a direct implication of Corollary 2.3, we have that the best decay rate is given by the spectral abscissa. As in the previous example, the hypotheses of Theorem 3.1 are satisfied for small enough damping terms $a(x)$. Following the idea of the experiments for the wave equation we considered the same damping functions $a(x)$. The results are almost identical to the previous cases (see Figure 7) and we omit them.

5.4. 2-D damped wave equation. We consider the square $\Omega = (0,1) \times (0,1)$ with boundary $\partial\Omega$, and the following system:

$$\partial_t^2 u(x,t) - \Delta u(x,t) + 2a(x)\partial_t u(x,t) = 0, \quad x \in \Omega,\ t > 0, \tag{5.18}$$

$$u(x,t) = 0, \quad x \in \partial\Omega,\ t > 0, \tag{5.19}$$

$$u(x,0) = u^0(x), \quad \partial_t u(x,0) = u^1(x), \quad x \in \Omega, \tag{5.20}$$

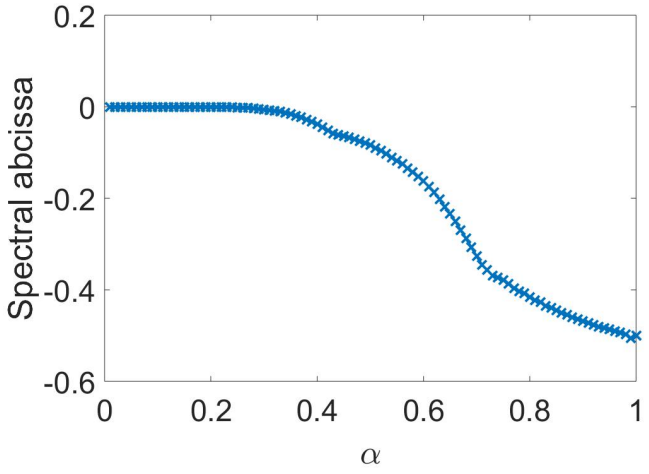

FIG. 8. *Spectral abscissa versus α for the 2-D damped wave equation when $a(x) = \frac{1}{\alpha^2}\chi_{D_\alpha}(x)$.*

where $a \in BV(\Omega)$ is nonnegative satisfying the following condition:

$$\exists\, c > 0 \text{ s.t. } a(x) \geq c \text{ a.e. in a nonempty open subset } I \text{ of } \Omega. \tag{5.21}$$

We define the energy of the solution u of (5.18)–(5.20), at time t, as

$$E\big(u(t)\big) = \frac{1}{2}\int_0^1 \left(\big|\partial_t u(x,t)\big|^2 + \big|\nabla u(x,t)\big|^2\right) dx\,, \tag{5.22}$$

$$U = L^2(\Omega),\ H = L^2(\Omega),\ H_{\frac{1}{2}} = H_0^1(\Omega),$$

$$\mathcal{D}(A) = H^2(\Omega) \cap H_0^1(\Omega), \quad \mathcal{H} = H_0^1(\Omega) \times L^2(\Omega),$$

$$A = -\Delta, \quad B\phi = B^*\phi = \sqrt{2a(x)}\phi \quad \forall \phi \in L^2(\Omega).$$

So,

$$\mathcal{A}_0 = \begin{pmatrix} 0 & I \\ \Delta & 0 \end{pmatrix},\ \mathcal{A}_{\mathcal{B}} = \begin{pmatrix} 0 & I \\ \Delta & -2a(x) \end{pmatrix}.$$

The operator $\mathcal{A}_0$ is skew-adjoint and with compact inverse and the spectrum is given by $\sigma(\mathcal{A}_0) = \left\{\pm i\sqrt{k^2+l^2}\pi, k, l \in \mathbb{N}^*\right\}$. Note that in this case the properties (A1)–(A2) are not satisfied. However, the spectral abscissa still provides an insight into the decay rate, at least when the support of the damping satisfies the so-called geometrical optics condition (see [18]).

The hypotheses of Theorem 3.1 are not satisfied in this case, but we try the numerical method anyway. Following the idea of the experiments for the 1-D wave equation we analyze the spectral abscissa for damping terms $a(x)$ that are characteristic functions of the form

$$a(x) = \frac{1}{\alpha^2}\chi_{D_\alpha}(x), \tag{5.23}$$

where $D_\alpha = (0.5 - \alpha/2, 0.5 + \alpha/2) \times (0.5 - \alpha/2, 0.5 + \alpha/2)$, and $\alpha \in (0, 1]$. Note that this is a characteristic function of a square that coincides with the domain for $\alpha = 1$ and approaches a Dirac mass as $\alpha \to 0$. The results are given in Figure 8. Note that in

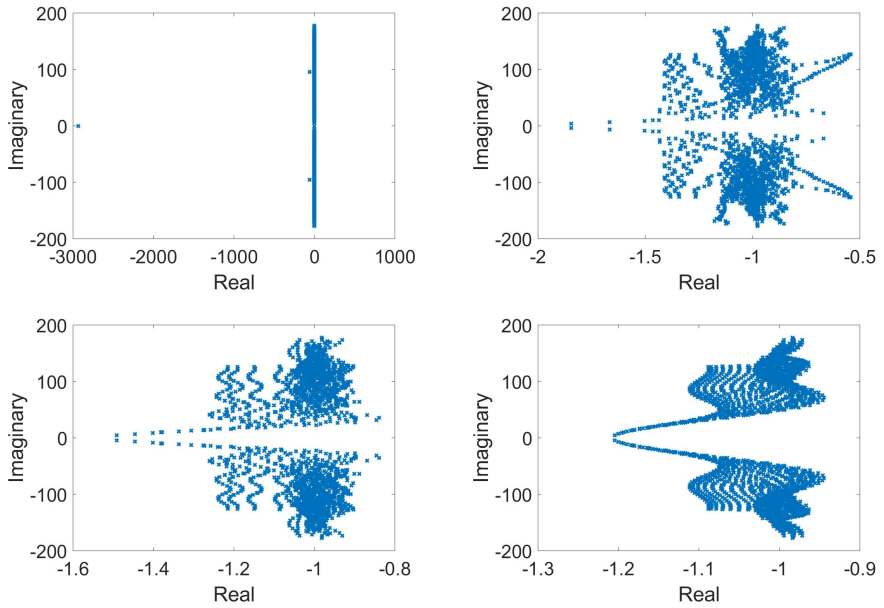

FIG. 9. *Spectrum of the 2-D damped wave equation when* $a(x) = \frac{1}{\alpha^2}\chi_{D_\alpha}(x)$ *for different values of* α*:* $\alpha = 0.01$ *(upper left),* $\alpha = 0.7$ *(upper right),* $\alpha = 0.8$ *(lower left), and* $\alpha = 0.9$ *(lower right).*

this case the support of the damping does not satisfy the geometrical optics condition and the decay rate at the continuous level can be larger than the spectral abscissa.

We observe that in this case, in contrast with the 1-D case, the spectral abscissa is monotone increasing when approaching the Dirac mass. In Figure 9 we show the spectrum in different cases.

Now we consider a two-parametric family of the form

$$a(x) = 64\chi_{D_{(\alpha_1,\alpha_2)}}(x), \qquad \alpha_1, \alpha_2 \in (1/16, 15/16),$$

where $D_{(\alpha_1,\alpha_2)}$ is the characteristic function of the $\frac{1}{8} \times \frac{1}{8}$ square centered at (α_1, α_2). Note that now the support of $a(x)$ is a square that we move through the domain Ω, along the two variables, and that we maintain the total mass at 1. The idea is to understand how the location of the damping affects the spectral abscissa. In Figure 10 we show the dependence on α. Note that it shows an oscillating behavior similar to the 1-D case.

6. Conclusions. We have introduced a projection method to approximate the spectrum of a dissipative system which is a bounded perturbation of a skew-adjoint operator. We show that the associated discrete spectra approximate the frequencies of the continuous problem uniformly with respect to the discretization parameter, up to a fixed number that can be estimated a priori. This is in contrast with other approaches, like the finite element method, for which the range of frequencies that are well approximated is difficult to estimate and, in general, depend on the discretization parameter.

Based on this result we introduce an algorithm to approximate the spectral abscissa, and therefore the decay rate, for a large class of dissipative systems. As applications we analyze the dependence of the damping location in several hyperbolic damped systems.

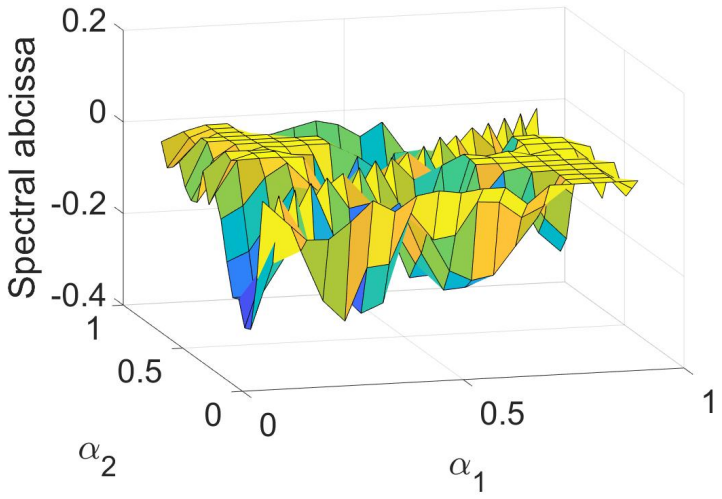

FIG. 10. *Spectral abscissa versus α for the 2-D damped wave equation when $a(x) = 64\chi_{D_{(\alpha_1,\alpha_2)}}(x), \alpha_1, \alpha_2 \in (1/16, 15/16)$. Here, $\alpha = (\alpha_1, \alpha_2)$ is the center of the support of the damping.*

Acknowledgment. The second author thanks Prof. E. Zuazua for his comments and suggestions that contributed to improve the presentation of this work.

REFERENCES

[1] K. AMMARI, M. DIMASSI, AND M. ZERZERI, *Stabilization of second order evolution equations by a class of unbounded feedback*, J. Differential Equations, 257 (2014), pp. 3501–3520.
[2] K. AMMARI, M. DIMASSI, AND M. ZERZERI, *Rate of decay of some abstract Petrowsky-like dissipative semi-groups*, Semigroup Forum, 93 (2016), pp. 1–16.
[3] K. AMMARI, A. HENROT, AND M. TUCSNAK, *Optimal location of the actuator for the pointwise stabilization of a string*, C. R. Acad. Sci. Sér. I Math., 330 (2000), pp. 275–280.
[4] K. AMMARI, A. HENROT, AND M. TUCSNAK, *Asymptotic behaviour of the solutions and optimal location of the actuator for the pointwise stabilization of a string*, Asymptot. Anal., 28 (2001), pp. 215–240.
[5] M. ASCH AND G. LEBEAU, *The spectrum of the damped wave operator for a bounded domain in $\mathbb{R}^2$*, Exp. Math., 12 (2003), pp. 227–241.
[6] C. CASTRO AND S. J. COX, *Achieving arbitrarily large decay in the damped wave equation*, SIAM J. Control Optim., 39 (2001), pp. 1748–1755.
[7] C. CASTRO AND S. MICU, *Boundary controllability of a linear semi-discrete 1-d wave equation derived from a mixed finite element method*, Numer. Math., 102 (2006), pp. 413–462.
[8] C. CASTRO, S. MICU, AND A. MÜNCH, *Numerical approximation of the boundary control for the wave equation with mixed finite element in a square*, IMA J. Numer. Anal., 28 (2008), pp. 186–214.
[9] S. COX AND E. ZUAZUA, *The rate at which energy decays in a damped string*, Comm. Partial Differential Equations, 19 (1994), pp. 213–243.
[10] S. COX AND E. ZUAZUA, *The rate at which energy decays in a string damped at one end*, Indiana Univ. Math. J., 44 (1995), pp. 545–573.
[11] S. ERVEDOZA AND E. ZUAZUA, *The wave equation: Control and numerics*, in Control of Partial Differential Equations, P. M. Cannarsa and J. M. Coron, eds. Lecture Notes in Math. 2048, Springer, Heidelberg, 2012, pp. 245–339.
[12] P. FREITAS, *Optimizing the rate of decay of solutions of the wave equation using genetic algorithms: A counterexample to the constant damping conjecture*, SIAM J. Control Optim., 37 (1999), pp. 376–387.

[13] R. Glowinski, C. H. Li, and J.-L. Lions, *A numerical approach to the exact boundary controllability of the wave equation* (i). *Dirichlet controls: Description of the numerical methods*, Jpn. J. Appl. Math., 7 (1990), pp. 1–76.
[14] R. Glowinski, J.-L. Lions, and J. He, *Exact and Approximate Controllability for Distributed Parameter Systems: A Numerical Approach*, Encyclopedia Math. Appl. 117, Cambridge University Press, Cambridge, 2008.
[15] A. Haraux, *Une remarque sur la stabilisation de certains systèmes du deuxième ordre en temps*, Port. Math., 46 (1989), pp. 245–258.
[16] T. J. Hughes, *The Finite Element Method. Linear Static and Dynamic Finite Element Analysis*, Prentice Hall, Englewood Cliffs, NJ, 1987.
[17] J. Infante and E. Zuazua, *Boundary observability for the space semi discretizations of the* 1*-d wave equation*, ESAIM Math. Model. Numer. Anal., 33 (1999), pp. 407–438.
[18] G. Lebeau, *Équation des ondes amorties*, in Algebraic and Geometric Methods in Mathematical Physics, Math. Phys. Stud., Kluwer, Dordrecht, The Netherlands, 1996, pp. 73–109.
[19] M. Negreanu and E. Zuazua, *Convergence of a multigrid method for the controllability of a* 1*-d wave equation*, C. R. Math., 338 (2004), pp. 413–418.
[20] J.-E. Osborn, *Approximation of the eigenvalues of non-selfadjoint operators*, Stud. Appl. Math., 45 (1966), pp. 391–401.
[21] K. Ramdani, T. Takahashi, and M. Tucsnak, *Uniformly exponentially stable approximations for a class of second order evolution equations*, ESAIM Control Optim. Calc. Var., 13 (2007), pp. 503–527.
[22] J. C. Strikwerda, *Finite Difference Schemes and Partial Differential Equations*, Chapman & Hall, New York, 1989.
[23] L. Thomson and P. Pinsky, *Complex wavenumber Fourier analysis of the p-version finite element method*, Comput. Mech., 13 (1992), pp. 255–275.
[24] G. Vainikko, *Evaluation of the error of the Bubnov–Galerkin method in an eigenvalue problem*, USSR Comput. Math. Math. Phys., 5 (1965), pp. 1–31.
[25] E. Zuazua, *Propagation, observation, and control of waves approximated by finite difference methods*, SIAM Rev., 47 (2005), pp. 197–243.